scientific reports

Check for updates

OPEN

GABA-mediated modulation of drought stress tolerance and seed morphology during flax (*Linum usitatissimum* L.) germination via image analysis

Selcuk Cetin[1] & Iskender Tiryaki[2]✉

Seed coat color, a trait exhibiting significant phenotypic variation, has been reported in previous studies to influence key germination parameters, including germination percentage, germination rate, and mean germination time. Looking into these relationships can help us identify plant varieties that better withstand both living threats and environmental challenges, which would make breeding programs more effective and focused. The objectives of this study were to evaluate the drought tolerance of 20 flax varieties at the germination stage, investigate the effects of gamma-aminobutyric acid (GABA) on seed germination performance under drought stress conditions, and explore potential associations between seed coat color and germination parameters under both stressed and non-stressed conditions using digital image processing. The final germination percentage, germination speed, and span of germination were assessed for seeds germinated under various germination conditions, including 23% PEG (− 0.169 MPa), 10 mM GABA, 23% PEG + 10 mM GABA, and a control treatment at 25 ± 0.5 °C. The results demonstrated substantial genetic variation across all germination parameters measured in the seeds of 20 distinct flax varieties. Genotype-specific responses to drought stress were observed, with 10 mM GABA alleviating the effects of drought. Among the varieties tested, Hermes exhibited the highest drought tolerance, while Lisette and Bonny-Doon were identified as drought-sensitive. Digital image processing analysis revealed significant differences ($p < 0.05$) in drought tolerance levels among flax varieties based on variations in RGB values of their seed coats. Although no statistically significant correlations were found in direct pairwise correlations between the color parameters converted from RGB (Red, Green, and Blue) to $L^*a^*b^*$ and germination parameters, multivariate PCA-biplot analysis indicated that L^* and b^* values had a positive influence on germination performance. In contrast, seeds with higher a^* values exhibited reduced germination performance. Furthermore, the biplot analysis suggested that varieties with lighter seed coats tended to show better germination compared to those with darker seed coats. These findings highlight the potential of incorporating seed coat color parameters into flax breeding programs, suggesting their role in enhancing seed germination and overall seed quality under various stress conditions.

Keywords Flax (*Linum usitatisstimum*), Drought, Gamma aminobutyric acid, Germination, Seed coat color, Image processing

Drought, resulting from global warming and climate change, leads to osmotic stress in plants, adversely affecting seed viability, germination rate, germination duration, root length, growth, and development[1], making it one of the most significant abiotic stress factors limiting agricultural production[2]. The duration of drought, the amount of water lost in cells, plant age, species, genotype, development, and the kind of cells or organs all have an impact on the biochemical, molecular, and physiological changes that occur in plant tissues[3], resulting in a defense mechanism against given stress conditions[4,5]. Plants have developed enzymatic and non-enzymatic antioxidant defense mechanisms to detoxify reactive oxygen species (ROS) produced as a result of oxidative stress [6,7]. The

[1]School of Graduate Studies, Canakkale Onsekiz Mart University, Terzioglu Campus, 17000 Çanakkale, Türkiye. [2]Department of Agricultural Biotechnology, Faculty of Agriculture, Canakkale Onsekiz Mart University, Terzioglu Campus, 17000 Canakkale, Türkiye. ✉email: tiryaki46@yahoo.com

production of ROS related enzymes or proteins on the seed coat may alter the color reflectance in the digital images and might diminish germination and early seedling growth stages, under severe stress circumstances[8–11].

Germination is a crucial seed quality parameter that directly affects plant yield and quality, fundamentally comprising two sub-attributes: the seed's ability to germinate and its capacity to sustain vigorous seedling emergence[12]. As one of the most critical stages in the plant life cycle, germination determines the growth of plants and their subsequent adaptation to various stress conditions[13]. However, under adverse environmental conditions, the germination potential of seeds is negatively impacted[14]. Exploring the genetic variety for drought tolerance is a vital step for selecting genotypes that perform better in water-stressed situations in various growth stages[15–18]. The detrimental effects of drought stress are known to vary depending on the genotype in many plant species[19]. Additionally, PEG-based screening has been shown to be an effective method for reliably identifying drought-tolerant or sensitive genotypes across various plant species[5,20,21]. However, it has been demonstrated that exogenous application of some compounds, metabolites, or plant growth regulators can mitigate the adverse consequences of drought stress. Exogenously administered 24-epibrassinoids, melatonin, and gamma-aminobutyric acid (GABA) enhance plant resilience to various conditions, including drought; GABA is a four-carbon molecule that is universally found in all living organisms[22–26]. While it functions as a neurotransmitter in animals and humans, it does not participate in protein synthesis[27,28]. GABA has been found to have roles in metabolic activities such as responding to abiotic and biotic stress stimuli, maintaining carbon/nitrogen (C/N) balance, and controlling plant growth and development[29–31].

Flax (*Linum usitatissimum* L.), used largely for oil and fiber production globally, is an important source of industrial raw materials[32]. Flax, like many cultivated plants is vulnerable to drought and high temperatures throughout the germination[33,34], seedling, and flowering stages[35,36]. Drought stress severely reduces the yield and quality of flax oil and fiber[37]. In addition to its use in the production of products such as medicines, dyes, biofuels, paper, clothing, and automotive parts[38], flax seeds contain polyunsaturated fatty acids (57% linolenic, 16% linoleic) and omega-3 (ω-3) fatty acids[39,40]. Due to their beneficial components for human health and rich antioxidant content[41,42], flax seeds are increasingly being consumed as an alternative plant-based food source to address health problems arising from changing dietary habits[43,44]. The structure and color of the seed coat are important not only for determining the quality and commercial value of the seeds[45], but also for revealing agricultural applications and seed germination parameters[40,46]. Recent studies have shown that computer vision and image processing techniques provide new and promising perspectives for the digital analysis of seeds by eliminating the limitations[47,48], and problems associated with traditional visual seed inspection, feature extraction, detection, or classification methods[49]. Therefore, the primary objectives of this study were threefold: (1) to elucidate the genetic diversity among 20 flax varieties subjected to polyethylene glycol (PEG_{6000})-induced drought stress during germination, (2) to investigate the influence of GABA on germination parameters of flax seeds under both drought-stressed and non-stressed conditions, and (3) to employ digital image analysis to assess potential relationships between seed coat color and germination characteristics.

Materials and methods

Seed materials

Seeds from 20 flax varieties, 10 oilseed varieties, and 10 fiber varieties were obtained from the Edirne Agricultural Research Institute (Türkiye). The information regarding the flax varieties used in this study is presented in Table 1.

Determination of PEG and GABA concentrations

To determine the optimal polyethylene glycol (PEG_{6000}) concentration for evaluating drought tolerance in 20 flax varieties, six PEG concentrations (20%, 21%, 22%, 23%, 24%, and 25%) were assessed on five representative flax varieties at 25 ± 0.5 °C. These concentrations corresponded to osmotic potentials of − 0.141, − 0.150, − 0.159, − 0.169, − 0.178, and − 0.188 MPa, respectively[50]. Experimental results demonstrated that a 23% PEG concentration, with an osmotic potential of − 0.169 MPa, was most suitable for subsequent drought tolerance assessments in the remaining 20 flax varieties (data not shown). In addition, to identify the most effective concentration of gamma-aminobutyric acid (GABA) for mitigating the inhibitory effects of PEG-induced drought stress on germination, a series of experiments were conducted using five flax varieties distinct from those employed in the PEG optimization study. Seven GABA concentrations (0.1, 0.5, 1, 3, 5, 7, and 10 mM) were evaluated. The results of these experiments demonstrated that 10 mM GABA was the most effective concentration and was therefore selected for subsequent experimental procedures (data not shown).

Germination experiments

In covered glass Petri dishes (60 × 15 mm), 25 seeds of each cultivar were arranged in a single layer on two layers of filter paper. A total of 4.5 mL of the previously determined optimal concentrations of 23% PEG, 10 mM GABA, or a combination of 23% PEG and 10 mM GABA was applied. Seeds treated with dH_2O served as the control. Germination experiments were conducted with four replications under constant dark conditions at a temperature of 25 ± 0.5 °C, as described previously[47]. Germination was defined as the emergence of a radicle measuring 1–2 mm. Seeds were monitored daily for 10 days, and the number of germinated seeds was recorded. Subsequently, final germination percentage (FGP), angular transformation of FGP data (arcsin√FGP), days to 50% of FGP (inverse measure of germination rate, G_{50}) and days between 10% and 90% of FGP (inverse measure of germination synchrony, G_{10-90}) were calculated[48]. The promotive effect of 10 mM GABA on FGP, the inhibitory effect of 23% PEG on FGP, and the recovery effect of 10 mM GABA under PEG-induced drought stress were determined based on the methodology described in the literature[48].

Registry code	Variety name	Intended use	Source
Lu1	Hermes	Fiber	Edirne Agricultural Research Institute
Lu2	Fivel	Fiber	Edirne Agricultural Research Institute
Lu3	Lisette	Fiber	Edirne Agricultural Research Institute
Lu4	Mures	Fiber	Edirne Agricultural Research Institute
Lu5	Eckendorfi	Fiber	Edirne Agricultural Research Institute
Lu6	Diana	Fiber	Edirne Agricultural Research Institute
Lu7	Merylin	Fiber	Edirne Agricultural Research Institute
Lu8	Suzanna	Fiber	Edirne Agricultural Research Institute
Lu9	Rolin	Fiber	Edirne Agricultural Research Institute
Lu10	Notajsa	Fiber	Edirne Agricultural Research Institute
Lu11	Crystal	Oilseed	Edirne Agricultural Research Institute
Lu12	Lackana	Oilseed	Edirne Agricultural Research Institute
Lu13	Bonny-Doon	Oilseed	Edirne Agricultural Research Institute
Lu14	Glenelg	Oilseed	Edirne Agricultural Research Institute
Lu15	Norman	Oilseed	Edirne Agricultural Research Institute
Lu16	Dillman	Oilseed	Edirne Agricultural Research Institute
Lu17	Miamara	Oilseed	Edirne Agricultural Research Institute
Lu18	Karakız	Oilseed	Edirne Agricultural Research Institute
Lu19	Sarı-85	Oilseed	Edirne Agricultural Research Institute
Lu20	Beyaz Gelin	Oilseed	Edirne Agricultural Research Institute

Table 1. Registry code, variety name, type of use and source of 20 flax varieties used in the study.

Creation of digital image dataset

A custom-designed photographic booth (dimensions: 30 cm × 30 cm × 30 cm) was employed to capture images of flax seeds. The booth featured adjustable light intensity and exposure height to optimize image quality. Image acquisition was performed using a 48-megapixel smartphone camera (Huawei P30, China), with a resolution of 6000 × 8000 pixels, an f/1.8 aperture, and a 75 mm super macro lens (Ulanzi, China). The imaging parameters were optimized as follows: ISO set to 800, shutter speed at 1/40 s, exposure value at 0°, and exposure height at 5 cm. Manual focus was applied (central, overhead), and the white balance was stabilized with a "Cloudy" setting to ensure consistent color representation.

For each flax variety, a total of 128 seeds were randomly selected to represent the seed lot. A dataset was generated by capturing 8 images, with 16 seeds included in each image. Sample images of the flax varieties are provided in Fig. 1.

Image processing for seed coat color analysis

Image processing techniques were employed to investigate the relationship between seed coat color and germination parameters under various germination conditions, utilizing images of flax varieties as depicted in Fig. 1. The primary objective of this step was to determine the digital seed coat color values (Red [R: 0–255], Green [G: 0–255], and Blue [B: 0–255]) for each flax variety. An image processing model was developed and implemented within the AugeLab Studio v2.2 software (AugeLab R&D Tech. Inc., Türkiye) environment, following the steps outlined below (Fig. 2). The image processing model was executed on a computer equipped with an AMD Ryzen 7 6800 H processor (4.75 GHz), 16 GB of RAM, and an Nvidia RTX 3050 Ti graphics card to ensure efficient processing.

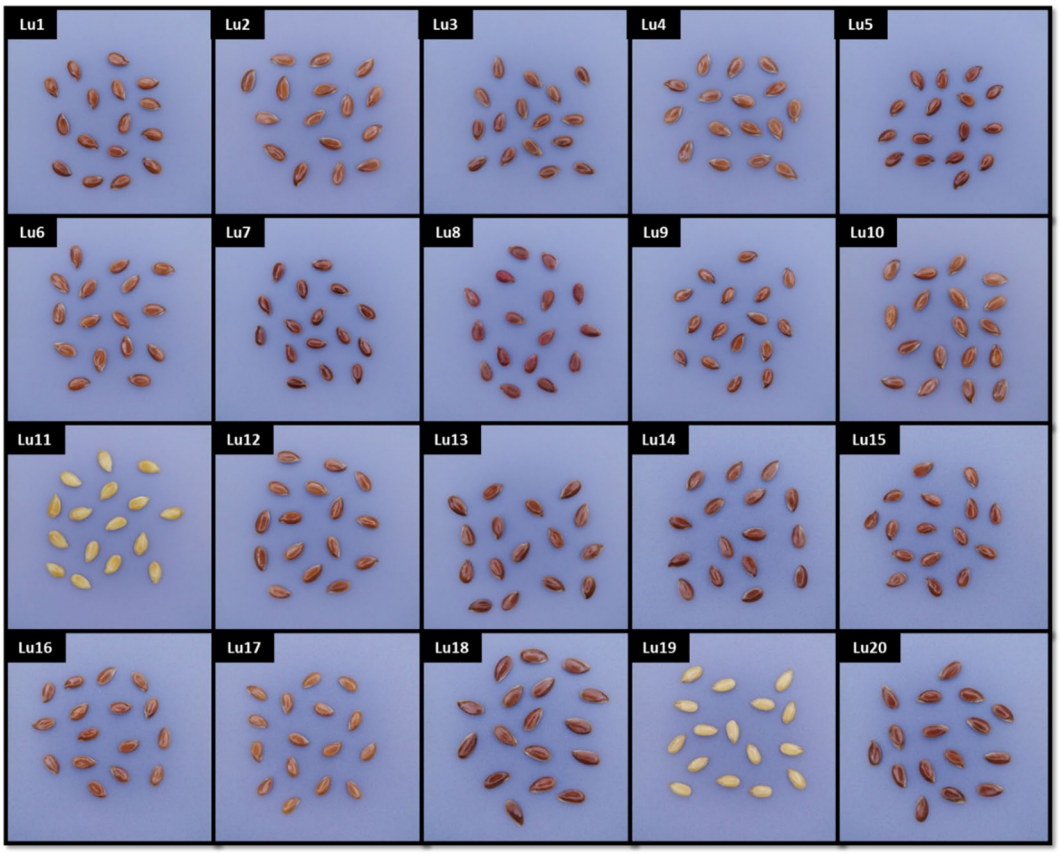

Fig. 1. Images of seeds from fiber (Lul - Lu10) and oilseed (Lu11 - Lu20) flax varieties.

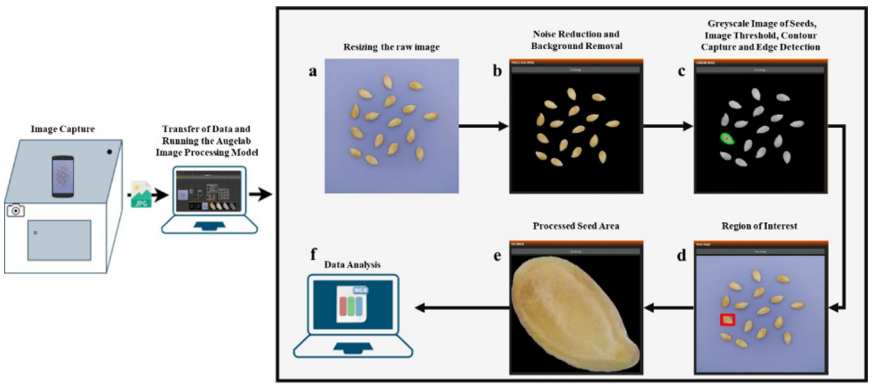

Fig. 2. The flow diagram illustrates the image processing model created for the segmentation of seeds and extraction of RGB color values using AugeLab Studio v2.2. The model incorporates several key steps to preprocess and analyze the seed images, ensuring accurate segmentation and color feature extraction. These steps include (1) Image capture: raw images of seeds were imported into the model; (2) Pre-processing: Initial image enhancements such as resizing, noise reduction, and background removal were applied; (3) Segmentation: The Otsu thresholding method is used to segment the seeds from the background, followed by contour detection to outline individual seeds; (4) Bounding Box Creation: A bounding box is created around each seed to define regions of interest (ROI); (5) RGB Pixel Calculation: The RGB color values for each seed are calculated by averaging the color values of non-black pixels within the ROI and (6) Data Analysis and Output: The segmented seeds and their corresponding average RGB color values were displayed for further analysis.

Image pre-processing

The key image pre-processing steps applied were presented in Fig. 2. To optimize the data by reducing noise, enhancing contrast, and improving the clarity of relevant features, raw images (resolution: 6000 × 8000 pixels) were first resized to 6000 × 6000 pixels using the image resizer block (Fig. 2a). To minimize noise while preserving

edge details, a bilateral filter was applied (Fig. 2b). An HSV filter was then applied with the following parameters: $Hue_{(min-max)}$: 84–150, $Saturation_{(min-max)}$: 0-255, and $Value_{(min-max)}$: 0-255, to isolate the blue background and convert it to black (RGB: 0–20) (Fig. 2b). Finally, the image was converted to a grayscale using the apply mask block (Fig. 2c).

Image segmentation and contour detection
To enhance the distinction of seed pixels in the grayscale image, the Otsu thresholding method[51], was applied. This technique automatically converts the image to a binary format by determining the optimal threshold value, effectively separating the seeds from the background (Fig. 2c). During the contour detection phase, the minimum contour area was set to range between 0% and 20% to identify and extract relevant contour areas in the image. This parameter adjustment allowed for the automatic generation of contour lines around each seed. Following this process, the total number of detected contours directly corresponded to the number of seeds in the image, as shown in Fig. 2c.

Feature extraction
In the feature extraction phase, a bounding box was generated around the detected contours for each seed, defining the minimum rectangular area (Fig. 2d). These bounding boxes, also referred to as regions of interest (ROI), were created by overlaying the original image, the background-extracted image, and the binary images. This approach facilitated the accurate detection of individual seeds and allowed for the precise definition of features to be processed in subsequent analysis steps (Fig. 2d).

Calculation of RGB pixels by removing background pixels
In the segmented image, the average values for the RGB channels were calculated separately for each pixel to simplify the color information. Black pixels, or background pixels, were found and eliminated from the analysis using a masking technique during the non-zero-pixel detection and masking process. In the subsequent size calculation phase, the number of RGB pixels within the identified regions of interest (ROI) was counted (Fig. 2e). To mitigate the influence of black pixels on the average RGB values within the ROI, the following formula was applied:

$$\text{Average RGB in ROI} = \frac{\text{ROI} \times \text{ Total pixel value in the ROI}}{\text{Total Number of RGB pixels}} \tag{1}$$

Extracting average RGB values of seeds
In the digital analysis of seed coat colors, the RGB channel information for each seed was calculated to quantitatively determine the color distribution on the seed surface. The color information was obtained by averaging the RGB values of each pixel while excluding black background pixels from the analysis to focus solely on the color characteristics of the seeds (Fig. 2e).

The following formulas were used to calculate the average R, G, and B color values for each seed:

$$\text{Red} = \frac{\text{RGB Pixel Count} \times \text{Average red value}}{\text{Number of black pixels}} \tag{2}$$

$$\text{Green} = \frac{\text{RGB Pixel Count} \times \text{Average red value}}{\text{Number of black pixels}} \tag{3}$$

$$\text{Blue} = \frac{\text{RGB Pixel Count} \times \text{Average blue value}}{\text{Number of black pixels}} \tag{4}$$

Color space conversion

To facilitate a more accurate and comparable analysis of the RGB values obtained from flax seed coats, the following color space transformations were applied.

Converting RGB to hexadecimal color space
The conversion of each RGB color value to a 16-based (hexadecimal-HEX) format enabled a more compact and interpretable representation of colors[52]. To convert RGB values to the hexadecimal color format, the following formulas were applied:

$$\text{R}_{\text{Hex}} = \frac{\text{Red}_{(0-255)}}{16} \tag{5}$$

$$\text{G}_{\text{Hex}} = \frac{\text{Green}_{(0-255)}}{16} \tag{6}$$

$$\text{B}_{\text{Hex}} = \frac{\text{Blue}_{(0-255)}}{16} \tag{7}$$

Within the framework of these formulas, if the remainder obtained by dividing the RGB values by 16 falls between 0 and 9, the value was written as a digit; however, if the remainder was between 10 and 15, it was represented by a letter from A to F (A = 10, B = 11, C = 12, D = 13, E = 14, F = 15). The resulting hexadecimal

color format was expressed using the #RRGGBB code, where RR, GG, and BB represent the hexadecimal values of the Red, Green, and Blue channels, respectively[53].

Converting RGB to XYZ color space

In the digital color system obtained through image processing, colors are typically represented in the RGB format. In contrast, spectrophotometric methods utilize the *L*a*b** reflection spectrum, which can be derived from the *XYZ* color space and is based on the International Commission on Illumination (CIE) system[54]. The *L*a*b** color system consists of three components the *L** axis represents lightness, ranging from black (0) to white (100); the *a** axis indicates color tones from green (-60) to red (+ 60); and the *b** axis represents color tones from blue (-60) to yellow (+ 60)[55,56]. Compared to the RGB or *XYZ* systems, the *L*a*b** system provides more detailed and perceptually uniform color information[54]. Unlike the RGB and *XYZ* color systems, the *L*a*b** system is designed to more closely mirror human visual perception of brightness and has been shown to be particularly effective in analyzing seed coat color and brightness[57–61]. Therefore, the RGB seed coat color values obtained through image processing were converted into the *XYZ* and *L*a*b** color systems, following the method outlined in the literature[62].

To convert RGB to *XYZ*, the RGB values were first normalized to a range between [0, 1]. For RGB [0, 1] normalization, the following formulas were applied:

$$R' = \frac{\mathrm{R}}{255}, \qquad G' = \frac{\mathrm{G}}{255}, \qquad B' = \frac{\mathrm{B}}{255} \tag{8}$$

To ensure more accurate color processing, the normalized RGB values were converted to a linear form through gamma correction[63]. The following formulas were used for the transformation:

If $R' \le 0.04045$, $G' \le 0.04045$, $B' \le 0.04045$ then;

$$R'' = \frac{R'}{12.92}, \quad G'' = \frac{G'}{12.92}, \quad B'' = \frac{B'}{12.92} \tag{9}$$

If $R' > 0.04045$, $G' > 0.04045$, $B' > 0.04045$ then;

$$R'' = \left(\frac{R' + 0.055}{1.055}\right)^{2.4}, \; G'' = \left(\frac{G' + 0.055}{1.055}\right)^{2.4}, \; B'' = \left(\frac{B' + 0.055}{1.055}\right)^{2.4} \tag{10}$$

To convert linear RGB values into the *XYZ* color space, the transformation matrix specified in the literature[64], was applied:

$$\begin{bmatrix} X \\ Y \\ Z \end{bmatrix} = \begin{bmatrix} 0.4124564 & 0.3575761 & 0.1804375 \\ 0.2126729 & 0.7151522 & 0.0721750 \\ 0.0193339 & 0.1191920 & 0.9503041 \end{bmatrix} \times \begin{bmatrix} R'' \\ G'' \\ B'' \end{bmatrix} \tag{11}$$

*Converting XYZ to L*a*b* color space*

To convert *XYZ* color space values to the *L*a*b* color space, the *XYZ* values were first normalized according to the 10° standard observer and the D65 reference white. For this normalization, the standard parameters of the CIE D65 reference white[65], were used, with values: *Xn* = 95.047, *Yn* = 100, and *Zn* = 108.883. The normalization process was carried out using the following formulas, as described in the literature[54]:

$$X_{norm} = \frac{X}{95.047}, \qquad Y_{norm} = \frac{Y}{100}, \qquad Z_{norm} = \frac{Z}{108.883} \tag{12}$$

To convert *XYZ* to *L*a*b* color space, the formulas outlined in the literature[66], were employed.

For the luminance axis (*L**), the calculation was as follows:

$$L^* = 116 \times f\left(\frac{Y}{Y_{norm}}\right) - 16 \tag{13}$$

For the *a** axis, the calculation was:

$$a^* = 500 \times \left(f\left(\frac{X}{X_{norm}}\right) - f\left(\frac{Y}{Y_{norm}}\right)\right) \tag{14}$$

For the *b** axis, the calculation was:

$$b^* = 200 \times \left(f\left(\frac{Y}{Y_{norm}}\right) - f\left(\frac{Z}{Z_{norm}}\right)\right) \tag{15}$$

These calculations rely on the function *f(t)*, defined as follows:

$$f(t) = \begin{cases} t^{\left(\frac{1}{3}\right)} & \text{if } t > \left(\frac{6}{29}\right)^3 \\ \frac{t}{3\left(\frac{6}{29}\right)^2} + \frac{4}{29} & \text{if } t \leqslant \left(\frac{6}{29}\right)^3 \end{cases} \quad (16)$$

Data analysis

Germination parameters, including final germination percentage (FGP), arcsin√FGP, germination speed (G_{50}), and germination span (G_{10-90}), were calculated as described previously[48]. The reduction in FGP under drought stress and the promotion and recovery effects of 10 mM GABA on FGP were calculated relative to the control values, following the methodology outlined in the literature[48]. The seed coat RGB values were determined using an image processing model developed by the authors, implemented through AugeLab Studio v2.2 software (AugeLab R&D Tech. Inc., Türkiye).

To enhance the visual interpretability of the seed coat colors obtained in the RGB format, the RGB values were converted to hexadecimal format, following the method outlined in the literature[53]. For a more accurate and comparable analysis, the RGB values were sequentially transformed into the *XYZ* color space according to the approach described in the literature[62], and subsequently converted into the CIE $L^*a^*b^*$ color space using the method recommended in the literature[66].

The $L^*a^*b^*$ values derived from the RGB data, collected in 8 replicates, were averaged and reduced to 4 replicates for use in correlation and biplot analysis. Statistical differences in the R, G, and B values of seed coats under different treatments, as well as the germination parameters, were assessed using analysis of variance (ANOVA) with Fisher's Least Significant Difference (LSD) test ($p < 0.05$).

Cluster analysis was performed independently to identify seed coat color similarities based on RGB values and to assess the relationships between germination parameters under various germination conditions. Pearson's correlation coefficients were used to analyze the relationships between germination parameters and seed coat $L^*a^*b^*$ values. Correlation analysis was conducted using JASP v0.19.1 Statistical Software[67]. Based on the correlation data, biplot analysis was conducted to evaluate and classify flax varieties across all parameters. ANOVA, biplot, and cluster analysis, along with their visualizations, were performed using Minitab Statistical Software[68].

Results

Seed germination parameters

All seed treatments exhibited significant ($p < 0.001$) effects, resulting in considerable variation in final germination percentage (FGP), germination speed (G_{50}), and germination span (G_{10-90}) among the flax varieties (Fig. 3). The genotype-dependent mitigation effects of GABA treatments on seeds germinated under control and drought conditions were quantified as percentage changes and are presented in Fig. 4. The FGP of seeds ranged from 78% to 100% under control conditions (Fig. 3a), with the inclusion of 10 mM GABA further increasing FGP values to between 94% and 100%. The lowest FGP (78%) under control conditions was observed in the variety of Lu8, which improved to 98% (17% increase in the FGP) with the addition of 10 mM GABA in non-stress conditions (Figs. 3a and 4). Conversely, a genotype-dependent drought response was observed under 23% PEG conditions (Figs. 3a and 4). The fiber variety Lu1 exhibited the lowest reduction in FGP due to drought stress, with a 21% decrease (Fig. 4). In contrast, the most sensitive varieties, Lu3 (fiber) and Lu13 (oilseed), showed complete germination inhibition (0% FGP) under PEG-induced drought stress (Figs. 3a and 4). The inclusion of 10 mM GABA in the 23% PEG medium (23% PEG + 10 mM GABA) significantly enhanced FGP across all flax varieties, with values ranging from 14% (Lu14) to 96% (Lu1) (Figs. 3a and 4). Notably, the previously non-germinating varieties, Lu3 and Lu13, achieved germination percentages of 64% and 16% in the presence of GABA, respectively (Fig. 4).

The time required to achieve 50% of the FGP (G_{50}) ranged from 0.85 days (Lu2 and Lu4) to 1.90 days (Lu8) under control conditions. The inclusion of 10 mM GABA exhibited a genotype-dependent effect on G_{50} values in non-stress conditions (Fig. 3b). For instance, G_{50} values were significantly reduced in varieties such as Lu8 and Lu11-Lu14, whereas they increased in Lu2 and Lu4 in response to 10 mM GABA (Fig. 3b). Under drought stress conditions, germination speeds were significantly slowed, increasing the time required to reach 50% of FGP across all flax varieties (Fig. 3b). However, the addition of 10 mM GABA generally had a positive effect on G_{50} values, mitigating the adverse impacts of drought stress (Fig. 3b).

All treatments showed significant variation ($p < 0.001$) in germination homogeneity (G_{10-90}) among the flax varieties (Fig. 3c). Under control conditions, the span of germination ranged from 1.25 days (Lu14) to 2.41 days (Lu11) (Fig. 3c). For seeds treated with 10 mM GABA in non-stress conditions, the G_{10-90} values varied between 1.54 days (Lu18) and 2.09 days (Lu20) (Fig. 3c). Drought stress induced by 23% PEG significantly ($p < 0.001$) increased G_{10-90} values across all genotypes, with few exceptions (Fig. 3c). The span of germination under drought stress ranged from 1.73 days (Lu1) to 4.33 days (Lu19). The mitigating effect of 10 mM GABA on induced drought stress varied significantly among the varieties tested (Fig. 3c). Overall, the seeds treated with 10 mM GABA under drought stress conditions exhibited more uniform germination compared to those germinated under drought stress alone (Fig. 3c).

Clustering analysis based on germination parameters

Hierarchical clustering analysis was performed to assess the similarities and differences among flax varieties based on the germination parameters examined under various germination conditions (Fig. 5). The complete linkage method and Euclidean distance metric were used to calculate the inter-cluster distances (Fig. 5). Under control conditions, the germinated flax varieties were grouped into two main clusters (Fig. 5a). The Lu8 variety was distinctly separated from the others, placing it in Cluster II. Cluster I was further subdivided into two sub-

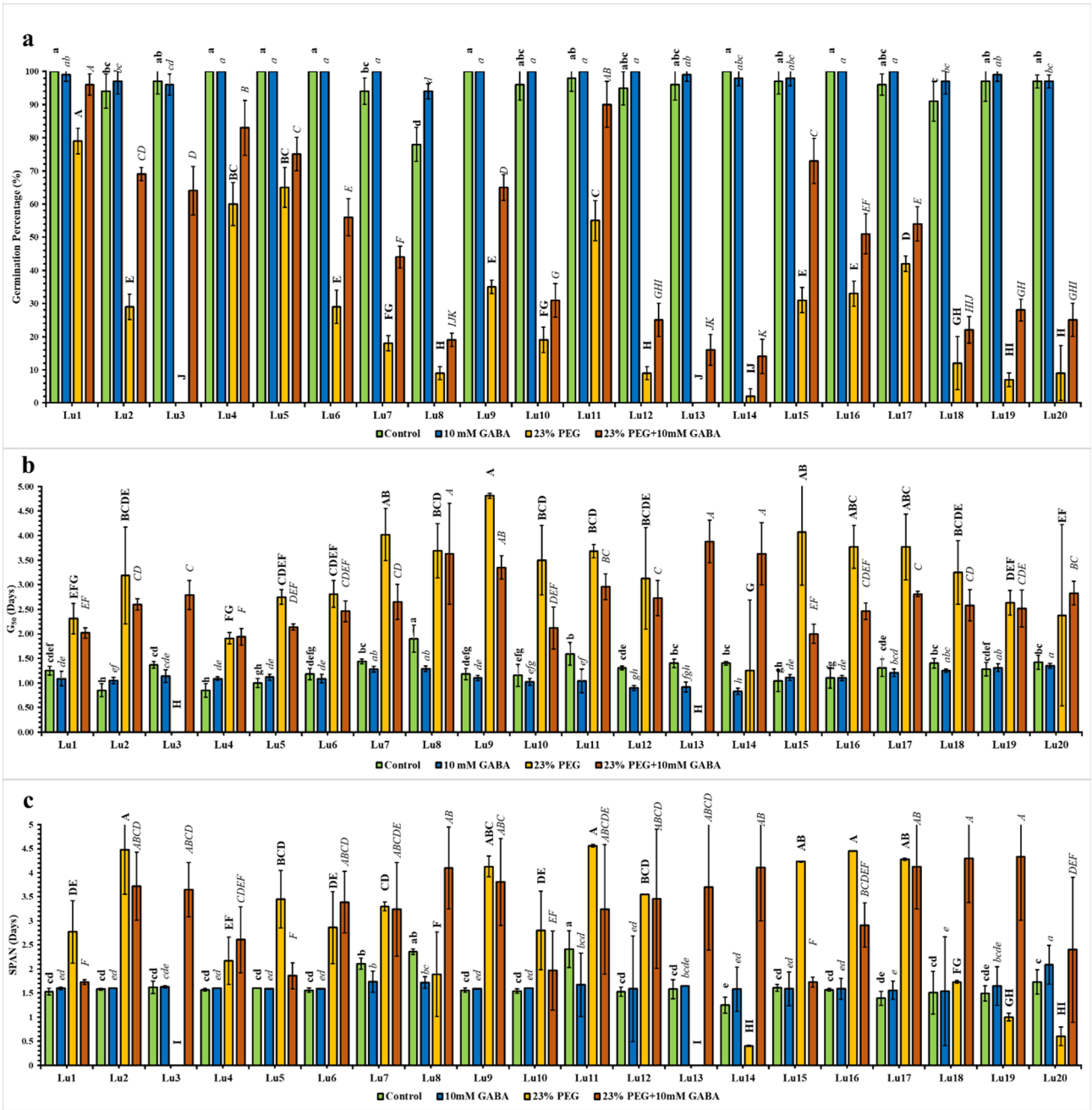

Fig. 3. Germination of seeds in the presence of 10 mM GABA, 23% PEG, 23% PEG + 10 mM GABA or dH_2O. (**a**) FGP, (**b**) G_{50}, and (**c**) span data for flax varieties. Vertical bars represent ± SE between replicates ($n = 4$). The same letters do not differ statistically at the $p < 0.05$ significance level. Capital, capital italic, small, or small italic letters indicate statistical analysis performed under given germination conditions.

clusters, IA and IB (Fig. 5a). Within Cluster I, sub-cluster IA was divided into two additional sub-clusters, IA-1 and IA-2. Varieties exhibiting high FGP and low G_{50} and span values, including Lu1, Lu4, Lu5, Lu6, Lu9, Lu10, Lu14, and Lu16, were grouped in sub-cluster IA-1 (Fig. 5a). Under non-stress conditions with the application of 10 mM GABA, the flax varieties were grouped into two main clusters: Cluster I (sub-clusters IA and IB) and Cluster II (sub-clusters IIA and IIB) (Fig. 5b). Varieties exhibiting high FGP and low G_{50} and span values were placed within sub-clusters IA and IB (Fig. 5b). In contrast, varieties with relatively low FGP values were clustered in Cluster II, where significant variation in FGP and span parameters was observed between the sub-clusters (Fig. 5b).

Varieties germinated under drought stress conditions were grouped into two main clusters (Cluster I and Cluster II), which were further subdivided into four sub-clusters: IA, IB, IIA, and IIB (Fig. 5c). The IA sub-cluster included varieties with the highest FGP under stress, such as Lu1 (79%), Lu4 (60%), Lu5 (65%), and Lu11 (55%) (Fig. 5c). In contrast, varieties with the lowest FGP values, including Lu3 (0%), Lu13 (0%), and Lu14 (2%), were

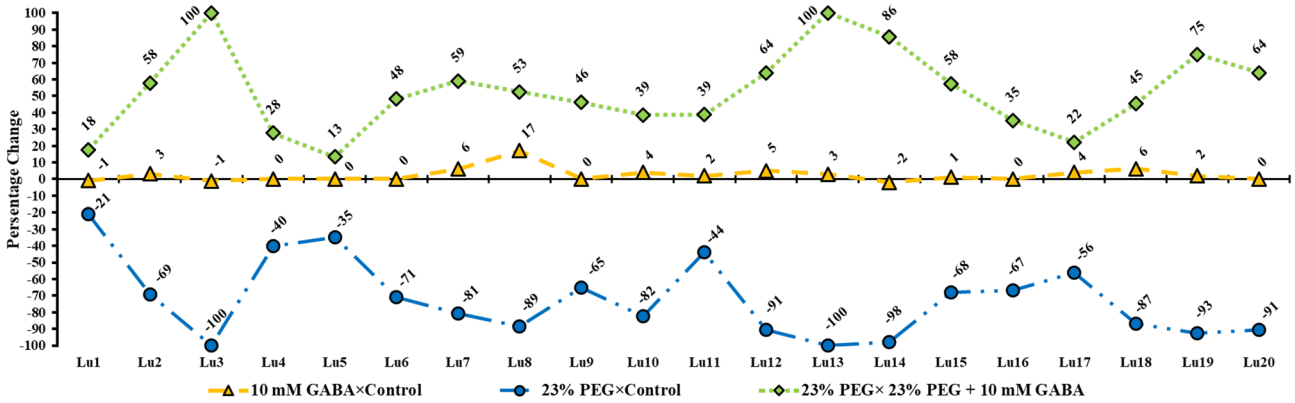

Fig. 4. Comparative graph of percentage changes on FGP due to given germination conditions.

placed in the IIA sub-cluster (Fig. 5c). The IB sub-cluster contained varieties with FGP values ranging from 29% to 42%, while the IIB sub-cluster included varieties with FGP values between 7% and 19% (Fig. 5c). Considerable variation in the germination parameters was observed among the clusters (Fig. 5c).

The seeds treated with GABA under drought stress conditions were divided into two main clusters (Cluster I and Cluster II), which were further subdivided into sub-clusters IA-IB and IIA-IIB (Fig. 5d). The two varieties with the highest FGP values, Lu1 (96%) and Lu11 (90%), were placed in the IA sub-cluster (Fig. 5d). The varieties with FGP values ranging from 83% to 64% were grouped in the IB sub-cluster, while those with FGP values between 56% and 44% were classified in the IIA sub-cluster (Fig. 5d). The varieties with FGP values between 3% and 16% were placed in the IIB sub-cluster. FGP values were the most significant parameter influencing the variation between clusters in the clustering analysis (Fig. 5d).

RGB analysis of seed coat color properties

Image processing analysis was utilized to quantitatively assess the color characteristics of the seed coat and to investigate the variation in seed coat color across flax varieties. For each variety, eight photographs were taken with 16 seeds, and the genetic variation in the red, green, and blue (R, G, B) color components obtained from these images was evaluated (Fig. 6). Statistical analysis revealed significant ($p < 0.001$) variation in seed coat color among the flax varieties (Fig. 6). The standard errors for the color values obtained through image processing ranged from 0.5 to 1.6 for red, 0.6 to 1.7 for blue, and 0.7 to 2 for green, indicating the success of the model and the optimizations performed. The red color channel was found to have the most significant influence on seed coat color (Fig. 6). The variety Lu7 exhibited the lowest RGB values (R: 112, G: 68, B: 65), while Lu19 displayed the highest color values (R: 199, G: 177, B: 137). Additionally, the varieties Lu13 and Lu20 showed identical RGB values for seed coat color (R: 123, G: 78, B: 72) (Fig. 6).

To examine the similarities and differences in RGB seed coat color among flax varieties, a clustering analysis was conducted using the complete linkage method and Euclidean distance metric (Fig. 7a). The analysis resulted in the division of flax varieties into two main clusters (Cluster I and Cluster II) based on their RGB seed coat color characteristics (Fig. 7a). The varieties with yellow seed coats, Lu11 and Lu19, were grouped in Cluster II, while those exhibiting various shades of brown were categorized into the sub-clusters IA and IB of Cluster I (Fig. 7a).

A three-dimensional scatter plot analysis based on RGB seed coat color data was performed to better understand the characteristics of the flax varieties in terms of their color components and to visualize their distributions (Fig. 7b). The resulting scatter plot depicted the relationships among the RGB color components of different varieties, revealing specific patterns and similarities (Fig. 7b). Additionally, the distribution of varieties based on RGB seed coat color aligned with the results obtained from the clustering analysis (Fig. 7b).

The data on seed coat color obtained in RGB format was converted to hexadecimal format, and the varieties were arranged from dark to light seed coat colors. This presentation offered a clearer and more perceptible depiction of the seed coat colors of the varieties (Fig. 8). The arrangement of varieties from dark to light seed coat colors was consistent with the distribution observed in the clustering analysis shown in Fig. 7.

Correlation analysis between germination parameters and *L*a*b** seed coat color

The Pearson correlation analysis between the germination parameters and the $L^*a^*b^*$ values of the seed coats of the varieties under various germination conditions was presented in Fig. 9. Under control conditions, significant correlations were observed among germination parameters and seed coat color values (Fig. 9a, Supplemental Table 1). Positive correlations included the span of germination and G_{50} ($r = 0.588$, $p < 0.01$) and L^* and b^* values ($r = 0.91$, $p < 0.001$). Negative correlations were identified between FGP and G_{50} (r = -0.623, $p < 0.01$), FGP and the span of germination (r = -0.535, $p < 0.05$), L^* and a^* values (r = -0.948, $p < 0.001$), and a^* and b^* values (r = -0.904, $p < 0.001$) (Fig. 9a, Supplemental Table 1). In seeds germinated in the presence of 10 mM GABA, significant positive correlations were observed between FGP and b^* ($r = 0.449$, $p < 0.05$), the span of germination and G_{50} ($r = 0.49$, $p < 0.05$), and L^* and b^* values ($r = 0.91$, $p < 0.001$) (Fig. 9b, Supplemental Table 2). Strong

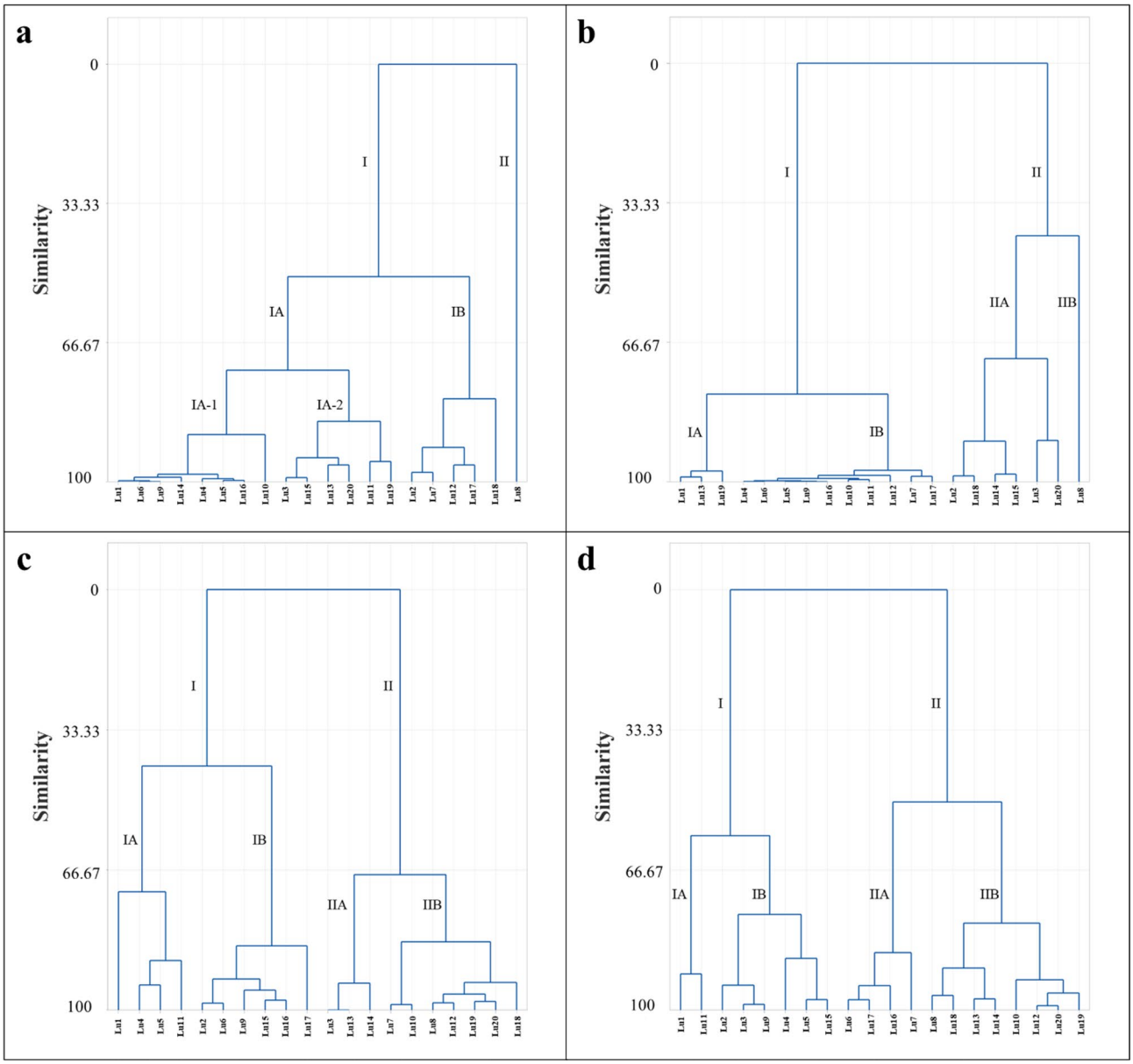

Fig. 5. Dendrogram illustrating the clustering status of flax varieties based on germination parameters under given germination conditions. (**a**) Control (dH_2O), (**b**) 10 mM GABA, (**c**) 23% PEG, **d**: 23% PEG + 10 mM GABA treatments.

negative correlations were also noted between L^* and a^* values (r = -0.948, $p < 0.001$) and a^* and b^* values (r = -0.904, $p < 0.001$).

Significant positive correlations were identified between FGP and the span of germination ($r = 0.585$, $p < 0.01$), G_{50} and the span of germination ($r = 0.802$, $p < 0.001$), and L^* and b^* values ($r = 0.910$, $p < 0.001$) (Fig. 9c, Supplemental Table 3) under drought stress conditions. Conversely, negative correlations were observed between L^* and a^* (r = -0.948, $p < 0.001$) and a^* and b^* (r = -0.904, $p < 0.001$) (Fig. 9c, Supplemental Table 3). Under drought stress conditions with the addition of 10 mM GABA, significant positive correlations were detected between the span of germination and G_{50} ($r = 0.666$, $p < 0.01$) and between L^* and b^* values ($r = 0.910$, $p < 0.001$) (Fig. 9d, Supplemental Table 4). Similarly, negative correlations were found between L^* and a^* (r = -0.948, $p < 0.001$) and between a^* and b^* (r = -0.904, $p < 0.001$) (Fig. 9d, Supplemental Table 4).

Differentiation of flax varieties based on $L^*a^*b^*$ seed coat color and biplot analysis under various germination conditions

A biplot analysis was performed to assess the variation in germination parameters and seed coat color ($L^*a^*b^*$) for seeds germinated under different conditions across 20 flax varieties (Fig. 10). This analysis provided a comprehensive visualization of the relationships between germination traits and seed coat color components, highlighting the multidimensional interactions among the measured parameters. The biplot effectively captured

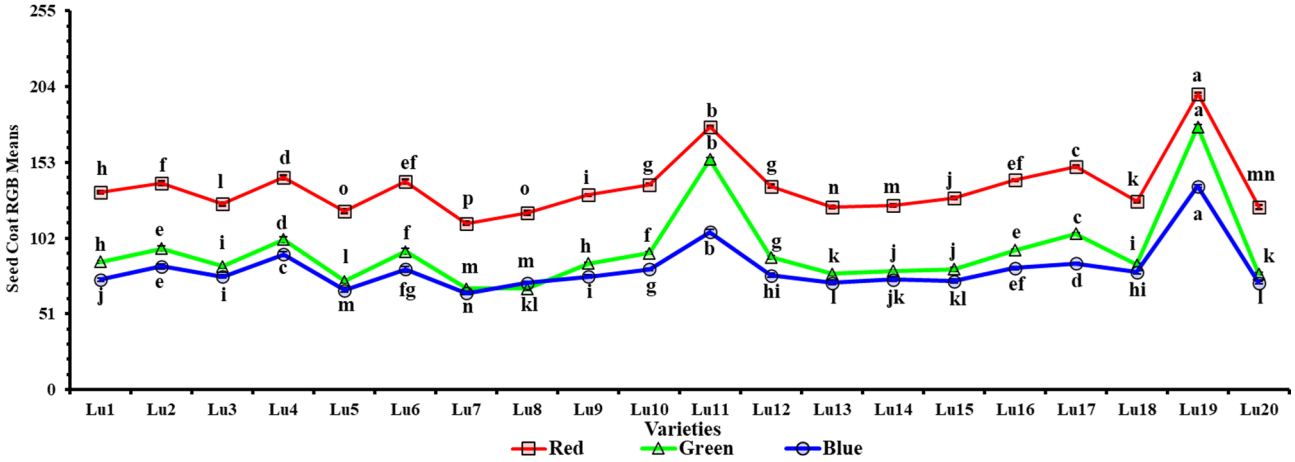

Fig. 6. The red, green, and blue color components of flax seed coats are presented. Vertical bars represent ± SE between replicates ($n = 8$). The same letters do not differ statistically at the $p < 0.05$ significance level.

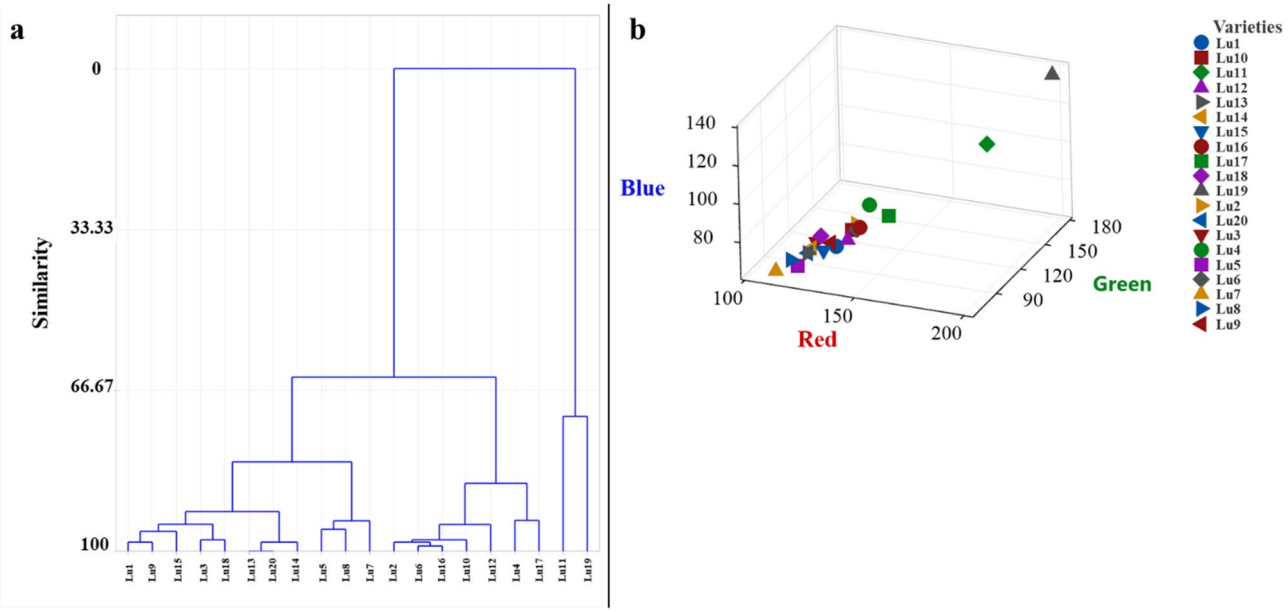

Fig. 7. Similarities and differences in RGB seed coat color among flax varieties. (**a**) Dendrogram showing the clustering of varieties (**b**) three-dimensional scatter plot illustrating the distribution of varieties.

the influence of germination conditions on the evaluated traits, offering insights into the variety differences and their responses to the experimental treatments. Under control conditions, the principal component analysis (PCA) revealed that the first two principal components (PC1 and PC2) accounted for 49.4% and 35.8% of the total variance, respectively, with a cumulative variance of 85.2% (Fig. 10a). The third and fourth components (PC3 and PC4) contributed to a cumulative variance of 92.2%, while the fifth and sixth components (PC5 and PC6) explained a smaller proportion of the variance (Supplemental Table 5). The PC1 demonstrated a strong association with the seed coat color parameters L^*, a^*, and b^*, with L^* exhibiting a positive loading (55.7%) (Fig. 10a, Supplemental Table 6). Conversely, a^* displayed a negative loading (-55.6%), while b^* showed a positive loading (56.0%) in PC1, indicating an inverse relationship between a^* and b^* (Fig. 10a, Supplemental Table 6). The PC2 was primarily associated with germination parameters, with FGP (52.5%) and G_{50} (59.2%) contributing positively, while the span of germination exhibited a significant negative loading (-58.4%) (Fig. 10a, Supplemental Table 6). This separation of germination parameters and seed coat color values across the PC1 and PC2 highlights their independence as distinct axes of variation (Fig. 10a, Supplemental Table 6). The PC3 was strongly associated with the span of germination, which contributed positively with a loading of 78.8%, while its relationship with other parameters was less pronounced (Supplemental Table 6). The PC4 showed a high positive association with G_{50} (70.4%), whereas FGP and the span of germination contributed less prominently to this

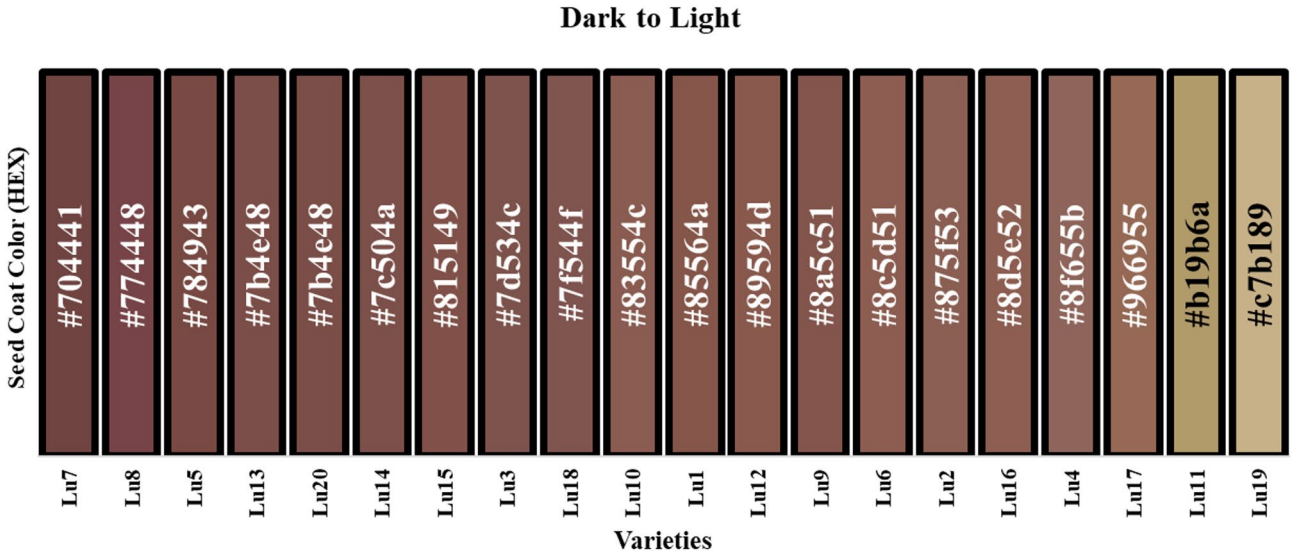

Fig. 8. Conversion of the RGB seed coat color of flax varieties to the hexadecimal color space, arranged from dark to light colors. The corresponding hexadecimal (HEX) color codes for each variety were provided within the bars.

component (Supplemental Table 6). The varieties Lu8, Lu11, and Lu19 were distinctly separated from the other varieties in the biplot analysis (Fig. 10a).

For the seeds germinated in the presence of 10 mM GABA, the analysis revealed that PC1 (50.6%) and PC2 (28.2%) together explained a cumulative variance of 78.8% (Fig. 10b). The contributions of PC3, PC4, PC5, and PC6 to the variance were 11.0%, 8.2%, 1.3%, and 0.7%, respectively (Supplemental Table 7), with PC5 and PC6 contributing minimally, accounting for only 1.3% of the total variance (Supplemental Table 7). The PC1 demonstrated a strong relationship with both seed coat color and germination parameters (Fig. 10b, Supplemental Table 8). Specifically, FGP was represented with a negative loading of -29.7% in PC1, while G_{50} exhibited a positive loading of 5.5% (Fig. 10b, Supplemental Table 8). The span of germination carried the highest negative loading of -81.2% in PC1, while seed coat colors represented by L^* and b^* were negatively loaded at -54.4% and −55.6%, respectively (Fig. 10b, Supplemental Table 8). In contrast, the a^* value was positively loaded (53.7%) in PC1 (Fig. 10b, Supplemental Table 8). These findings highlight the significant influence of seed germination parameters on seed coat color within PC1. The PC2 showed a notable relationship with germination parameters (Fig. 10b, Supplemental Table 8). The G_{50} had a high positive loading of 64.8% in PC2, while span was represented with a negative loading of -59.9% (Fig. 10b, Supplemental Table 8). The FGP contributed less (5.5%) to this component, further emphasizing the separation of germination parameters and seed coat color values into two independent principal components (Fig. 10b, Supplemental Table 8). The PC3 exhibited a high positive relationship, particularly with the span of germination (78.8%), while its relationships with other parameters remained lower (Supplemental Table 8). The PC4 was predominantly represented by G_{50} with a positive loading of 74.2%, whereas FGP and the span of germination had lower loadings in this component (Supplemental Table 8). The varieties Lu8, Lu11, Lu19 and Lu20 were distinctly separated from the other varieties in the biplot analysis (Fig. 10b).

Under drought stress conditions, the first two principal components (PC1 and PC2) explained a total variance of 83.9%, with PC1 accounting for 51.1% and PC2 contributing 32.8% (Fig. 10c). The third (PC3) and fourth components (PC4) together explained a cumulative variance of 95.9%, while the contributions of the fifth (PC5) and sixth components (PC6) were minimal, accounting for only 4.1% (Supplemental Table 9). The PC1 demonstrated a significant relationship with both seed germination parameters and seed coat color (Fig. 10c). The FGP parameter was represented with a positive loading of 24.8% in PC1, while G_{50} exhibited an influence of 22.7% (Fig. 10c, Supplemental Table 10). The span of germination showed a positive loading of 29.3% in PC1 (Fig. 10c, Supplemental Table 10). Among seed coat color variables, L^* exhibited the highest positive loading of 51.1%, while a^* showed a negative loading of -49.3% (Fig. 10c, Supplemental Table 10). These results clearly indicated the combined effect of seed germination parameters and seed coat color on PC1. The PC2 demonstrated a strong relationship with germination parameters (Fig. 10c). The G_{50} contributed significantly with a loading of 53.9% in PC2, while the span of germination showed a high positive loading of 58.0% (Fig. 10c, Supplemental Table 10). The FGP had a relatively lower influence, with a contribution of 39.8% in PC2 (Supplemental Table 10). These findings suggest that germination parameters and seed coat color values are distinguishable within PC2. The varieties Lu11 and Lu19 were distinctly separated from the other varieties in the biplot analysis (Fig. 10c). The PC3 exhibited a high negative relationship with FGP (81.9%), while its relationship with other parameters remained lower (Supplemental Table 10). The PC4 was characterized by a notable negative loading with the span of germination (-62.6%) (Supplemental Table 10).

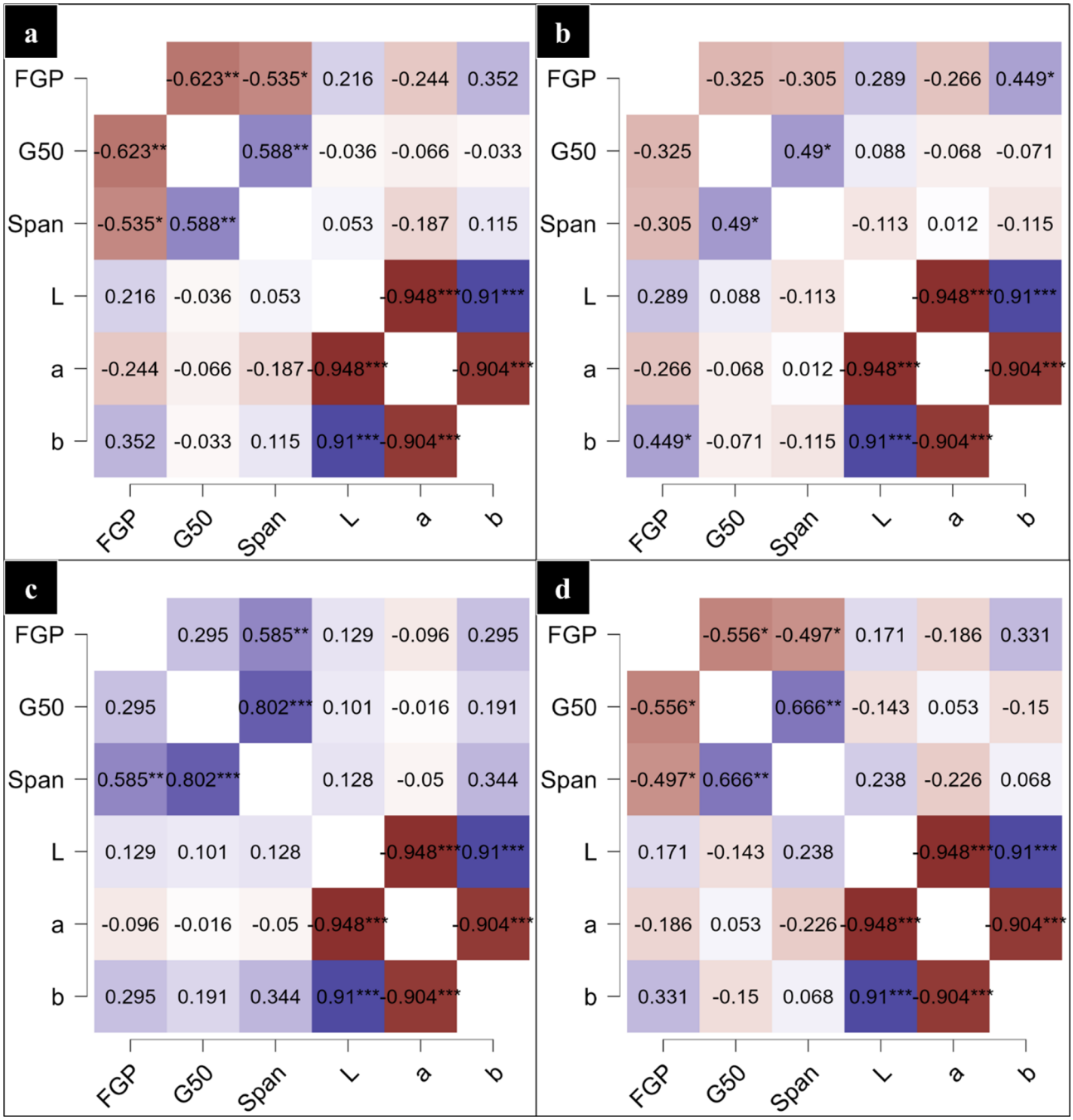

Fig. 9. Correlation matrix between germination parameters of 20 flax varieties examined under various germination conditions and the $L^*a^*b^*$ seed coat color. (**a**) Control (dH_2O), (**b**) 10 mM GABA, (**c**) 23% PEG, (**d**) 23% PEG + 10 mM GABA treatments. FGP: final germination percentage; G_{50}: germination rate; Span: germination homogeneity; L^*: lightness; a^*: green/red; b^*: blue/yellow. Each square represents the Pearson's correlation coefficient for a pair of parameters. Correlation coefficients are significant at $^*p < 0.05$, $^{**}p < 0.01$, and $^{***}p < 0.001$ levels. Shades of blue and red indicate positive and negative correlations, respectively.

Under drought stress conditions combined with 10 mM GABA treatment, the first two principal components (PC1 and PC2) accounted for a total variance of 85.2%, with PC1 explaining 49.6% and PC2 contributing 35.6% (Fig. 10d). The third (PC3) and fourth (PC4) components together explained a cumulative variance of 93.1%, while the contributions of the fifth (PC5) and sixth components (PC6) were minimal, accounting for 6.1% (Supplemental Table 11). In PC1, FGP exhibited a positive loading of 22.3%, while the a^* value had a negative loading of -55.2% (Fig. 10d, Supplemental Table 12), indicating a strong influence of seed coat color on FGP. The L^* value provided the highest positive contribution, with a loading of 55.7%, and b^* also contributed significantly with a positive loading of 55.9% (Fig. 10d, Supplemental Table 12). The PC2 displayed a strong relationship with

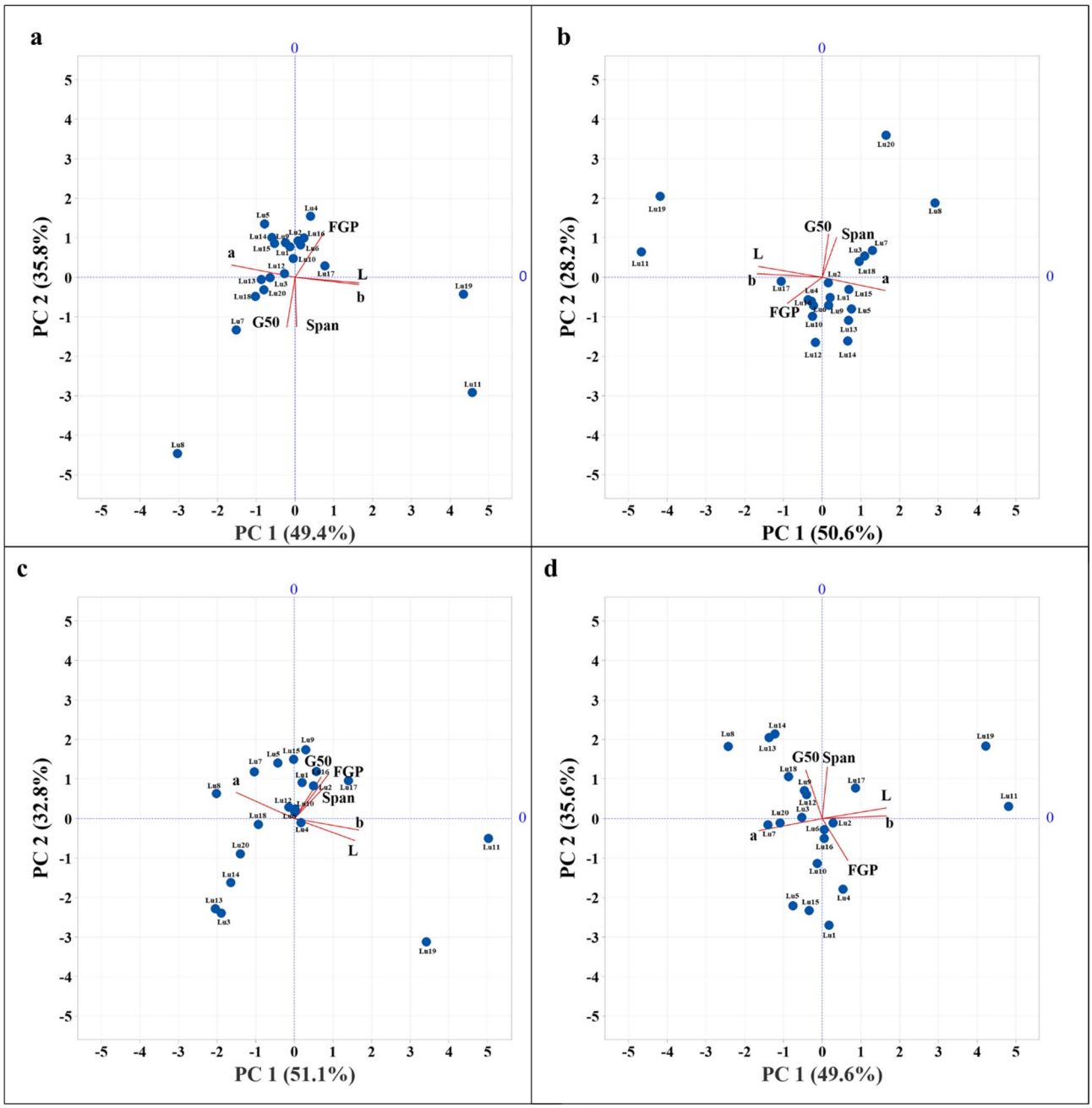

Fig. 10. Biplot showing the distribution of 20 flax varieties in relation to germination parameters and $L^*a^*b^*$ seed coat color under various germination conditions. (**a**) Control (dH_2O), (**b**) 10 mM GABA, (**c**) 23% PEG, (**d**) 23% PEG + 10 mM GABA treatments. FGP: final germination percentage; G_{50}: germination rate; span: germination homogeneity; L^*: lightness; a^*: green/red; b^*: blue/yellow. Blue dots represent the varieties.

germination parameters, with G_{50} showing a positive loading of 57.9% and the span of germination contributing 61.5% (Fig. 10d, Supplemental Table 12). In contrast, the FGP had a negative loading of -49.9% in PC2 (Fig. 10d, Supplemental Table 12), further suggesting a distinction between germination parameters and seed coat color measurements. The PC3 demonstrated a high positive loading with FGP (81.0%), while its relationships with other parameters were relatively weaker (Supplemental Table 12). The PC4 showed a prominent relationship with the span of germination (71.6%), whereas G_{50} exhibited a negative loading of -59.3% (Supplemental Table 12). The varieties Lu11 and Lu19 were distinctly separated from the other varieties in the biplot analysis (Fig. 10d). These findings underscore the separation between seed germination parameters and seed coat color components in the principal component analysis.

Discussion

Seed germination is a critical stage in plant production, serving as a prerequisite for subsequent growth and development. However, drought stress negatively impacts germination[69,70], and can lead to yield losses ranging from 55% to 92%, depending on the plant species, variety, or genotype[71]. Consequently, the development of plant species/genotypes that are minimally affected or unaffected by drought stress has become a primary objective of global breeding programs[72,73]. Previous studies have demonstrated that PEG-induced drought stress is an effective tool for identifying drought-tolerant and sensitive varieties/genotypes, provided that drought conditions were properly adjusted for the specific crop plants being studied[7,74,75]. Therefore, a critical consideration in such studies is the determination of a practical or ecologically relevant threshold for drought tolerance. This highlights the necessity of precisely optimizing the PEG concentration to achieve two key objectives: maximizing the differentiation of tolerance levels among varieties while ensuring germination in tolerant genotypes and effectively distinguishing highly tolerant genotypes within the tolerant group. In this study, a germination rate exceeding 50% under the selected PEG concentration was employed as the threshold for classifying genotypes as drought tolerant. This threshold, relevant for practical agricultural applications, effectively discriminates between tolerant and sensitive genotypes. This approach provides a robust and crucial criterion for evaluating genotype performance in drought tolerance assessments. Current research highlights the significance of these conditions and the evaluation parameters, such as germination percentage, speed, and span of germination, in assessing drought tolerance level of 20 flax varieties. PEG is widely recognized for its inability to pass through the cell wall due to its high molecular weight. PEG influences the water potential of embryonic cells by restricting water flow from the xylem to adjacent cells, thereby limiting cell growth primarily through the loss of turgor pressure[50]. This results in impaired cell elongation and inhibition of seed germination[76]. The results of this study indicated that an optimized PEG concentration of 23%, yielding an osmotic potential of − 0.169 MPa at 25 ± 0.5 °C, effectively differentiated drought responses among 20 flax varieties (Fig. 3a). This finding corroborates previous research demonstrating that a 20% PEG concentration, with an osmotic potential of − 0.169 MPa, at 20 °C was sufficient to distinguish between drought-sensitive and drought-tolerant flax genotypes[33]. Germination percentages under PEG-induced drought stress conditions varied substantially, ranging from 79% (Lu1) to 0% (Lu3 and Lu13), further emphasizing the significant genetic diversity in drought tolerance within the flax varieties tested (Fig. 3a). Variations in germination under drought stress induced by PEG have been observed in other important crops, including alfalfa[7,77], clover[78], and wheat[79].

The results of this study provided the first evidence that GABA significantly improved seed germination parameters in flax varieties, with the effect being genotype-dependent, under both stress and non-stress conditions (Figs. 3 and 4). The Lu8 variety, which exhibited a germination percentage of 78% under control conditions, showed a significant increase of 17% following GABA treatment, achieving a FGP of 94% (Figs. 3a and 4). Moreover, the application of 10 mM GABA under non-stress conditions generally enhanced both the speed and extent of germination across the flax varieties (Figs. 3 and 4). Drought stress led to considerable reductions in the FGP of the varieties, but the inclusion of 10 mM GABA alleviated the stress and significantly improved all germination parameters assessed (Figs. 3 and 4). However, the degree of recovery induced by GABA varied among the varieties. For example, the Lu3 and Lu13 varieties, which exhibited an FGP of 0% under drought stress, demonstrated a substantial increase in germination, with FGP of 64% and 16%, respectively (Figs. 3a and 4). These findings are consistent with previous studies highlighting the positive effects of GABA on seed viability and germination performance under stress conditions[80–82]. Numerous studies have also highlighted the critical role of GABA in enhancing stress tolerance in plants, primarily through the regulation of the tricarboxylic acid cycle, nitrogen reserves, cytoplasmic pH, antioxidant defense mechanisms, and osmotic potential[83,84]. Clustering analysis based on germination parameters effectively differentiated drought-tolerant and drought-sensitive varieties, grouping them within the same subgroups under drought stress conditions (Fig. 5c-d). Similar clustering patterns were observed under non-stress conditions, revealing both the similarities and differences among the flax varieties (Fig. 5a-b). Interestingly, the drought response and GABA effects were not influenced by the fiber or oil type of the flax varieties. The most drought-tolerant variety, Lu1, was identified as a fiber type, while the drought-sensitive varieties, Lu3 and Lu13, were classified as fiber and oil types, respectively (Figs. 3 and 4).

The seed coat, which forms the outermost layer of the seed, serves as a protective barrier against both biotic and abiotic factors, plays a crucial role in water absorption, and provides resistance to physical impacts[85]. Seed coat properties, such as color, brightness, and thickness, are established at the physiological maturity stage, and seed coat pigmentation has been shown to play a crucial role in regulating seed dormancy and germination traits[40,57,86,87]. Seed coat color is also a central target in many plant species, and any characteristic associated with it is crucial for selecting or not selecting desired or undesired plant material in a breeding program[57,86,87]. It has been reported that seed coat color is linked to various characteristics related to seed yield and quality, making these characteristics key targets for breeding studies[88–91]. In this study, the seed coat colors of flax varieties were quantified in RGB format through the image processing model of AugeLab Studio software v2.2 (AugeLab R&D Tech. Inc., Türkiye), which is an innovative and user-friendly platform designed to streamline artificial intelligence (AI) and image processing workflows without the need for coding expertise. The results of image processing analysis indicated that the Lu13 and Lu20 varieties displayed identical RGB-defined seed coat colors, while significant differences were observed among the remaining varieties (Fig. 6). Clustering analysis based on RGB seed coat color revealed both similarities and differences among the varieties (Fig. 7a-b). The analysis showed that Lu11 and Lu19, which possess yellow seed coats, clustered separately, thereby clearly distinguishing them from the other varieties (Fig. 7a). Furthermore, the conversion of seed coat RGB values to hexadecimal format resulted in a color gradient ranging from dark to light, which was consistent with the clustering analysis outcomes (Fig. 8).

Under various germination conditions, although positive or negative correlations were observed between seed germination parameters (FGP, G_{50}, and Span) and seed coat color (L^*, a^*, and b^*), these correlations were not statistically significant (Fig. 9). Furthermore, biplot analyses clearly demonstrated that the relationship between germination parameters and seed color traits varied across the different germination conditions. For instance, under control conditions, PC1 was significantly influenced by the color parameters L^* (0.557), b^* (0.560), and a^* (-0.556) (Fig. 10a, Supplemental Table 6). This suggests that the L^* value, which represents the degree of light reflection, and the b^* value, reflecting bluish-yellow tones, positively contribute to PC1 (Fig. 10a). The varieties Lu11 and Lu19, which exhibited the most bluish-yellow seed coat colors with hexadecimal color values of #b19b6a and #c7b189, respectively (Fig. 8), were distinctly separated from the other varieties. These two varieties were positioned in the same direction as L^* and b^* in the biplot (Fig. 10a). Conversely, the negative influence of the a^* value, representing the reddish-green balance, is noteworthy. The findings indicated that seeds with higher a^* values (reddish) could adversely affect germination performance (Fig. 10a). Although the FGP (0.250) and span (0.013) contributed positively to PC1, their contributions remained low (Supplemental Table 6). In contrast, PC2 was shaped primarily by span (-0.584) and G_{50} (-0.592), with these two parameters being the main factors negatively affecting PC2 (Fig. 10a, Supplemental Table 6). This evidence suggests a relationship, particularly between the germination speed (G_{50}), the span of germination (G_{10-90}), and PC2. The conclusion was further supported by the observation that varieties such as Lu3, Lu7, Lu8, Lu18, and Lu20, which cluster in this region of the biplot, generally exhibited slow and extended germination patterns (Figs. 3b-c and 10a). These varieties were also categorized in the middle-left part of the classification based on hexadecimal color values (Fig. 8). However, the results revealed that the parameters of seed coat color on germination parameters under control conditions was limited.

The seeds treated with 10 mM GABA under no stress conditions: PC1 and PC2 explained a total variance of 78.9% (Fig. 10b). The largest loadings on PC1 again came from L^* (-0.544), a^* (0.537), and b^* (-0.556) values (Fig. 10b, Supplemental Table 8). Interestingly, the L^* and b^* values exhibited negative effects on PC1 under GABA application, which was contrary to control conditions (Fig. 10a-b). This suggests that the contribution of GABA to total variation may negatively affect seeds with lighter, bluish-yellow coat colors under non-stress conditions. This hypothesis is further supported by the placement of the Lu11 and Lu19 varieties along the same direction as the L^* and b^* values on the biplot (Fig. 10b). The germination parameters, including FGP (-0.297), G_{50} (0.055), and span (0.123), exhibited weak effects on PC1 (Fig. 10b, Supplemental Table 8). In contrast, G_{50} (0.648) and span (0.599) displayed high positive loadings on PC2, suggesting a significant influence of GABA on the speed and span of germination (Fig. 10b, Supplemental Table 8). These findings may indicate that GABA may enhance seed germination performance, particularly in seeds characterized by lower L^* (darker) and b^* (more yellowish) values, when germinated under non-stress conditions.

Under 23% PEG-induced drought stress conditions, the strongest loadings in PC1 were observed for L^* (0.511) and b^* (0.545), while the a^* value (-0.493) exhibited a negative effect (Fig. 10c, Supplemental Table 10). These results suggest that under drought stress, lighter-colored and bluish-yellow seed coats positively influence germination, whereas reddish seed coats (indicated by a high a^* value) have a detrimental effect (Fig. 10c). In terms of germination parameters, both FGP (0.248) and G_{50} (0.227) showed positive contributions to PC1, aligning with the color parameters (Fig. 10c, Supplemental Table 10). Varieties with similar hexadecimal color values were grouped together in the biplot, demonstrating consistent patterns (Figs. 8 and 10c). However, span (0.580) exhibited one of the strongest loadings in PC2, emphasizing its more pronounced role under drought stress conditions (Fig. 10c, Supplemental Table 10).

In the presence of 10 mM GABA under drought stress, the largest loadings in PC1 were carried by L^* (0.557), a^* (-0.552), and b^* (0.559) (Fig. 10d, Supplemental Table 12). A positive relationship between lighter and bluish-yellow seed coat colors (higher L^* and b^* values) and germination parameters was observed in this condition (Fig. 10d). Conversely, as in other conditions, the a^* value representing red tones exerted a negative influence (Fig. 10d). In terms of germination parameters, FGP (0.223) had a positive effect on PC1, while G_{50} (-0.144) showed a negative effect (Fig. 10d, Supplemental Table 12). Notably, under drought stress with 10 mM GABA, the time to 50% of FGP (G_{50}) negatively impacted FGP, whereas the overall germination rate (FGP) was enhanced (Fig. 10c-d). The span of germination (0.615) exhibited the highest positive loading in PC2, indicating that the distribution of varieties was primarily determined by this component (Fig. 10d, Supplemental Table 12).

Flax seeds vary in size from 4 to 6 mm in length and 2 to 3 mm in width, exhibiting a color scale of brown and yellow tones in their seed coat[92]. It has been reported that flax seed coat color is linked to various characteristics related to seed yield and quality[40,88,89,91,93]. As the seed coat color transitions from yellow to brown, there is an increase in seed coat thickness, making it tougher[94]. Additionally, the darkening of the seed coat is associated with higher levels of oil, tannins, secondary metabolites, and antioxidant compounds, suggesting that brown seeds exhibit greater drought tolerance than yellow seeds[40,89,94,95]. In flax varieties with darker seed coats, a more significant increase in lignan biosynthesis has been observed under drought stress compared to yellow-coated varieties, indicating that this increase plays a key role in enhancing the plant's drought tolerance[40,96]. In the current study, the observed decline in germination parameters in seeds with darker brown seed coats, compared to those with lighter brown or yellow coats, is likely due to differences in genetic background. Another contributing factor may be the thicker seed coat structure of the darker brown seeds[92], which could restrict water absorption under drought stress conditions, as compared to the thinner seed coats of lighter brown or yellow seeds.

Conclusions

The seeds of 20 different flax varieties exhibited significant variation in germination parameters under various germination conditions. Genotype-dependent effects of drought stress were observed, with 10 mM GABA mitigating the impact of drought stress. Among the varieties, Hermes (Lu1) was identified as the most drought-

tolerant, while Lisette (Lu3) and Bonny-Doon (Lu13) were found to be drought-sensitive. The image processing model developed in this study, utilizing a photography chamber and exposure optimizations, proved capable of detecting seed coat color at a lower cost and with greater speed in comparison to established seed color testing methods. No significant correlation was observed between the color parameters (L^*, a^*, and b^*) derived from RGB values and the germination parameters measured in this study.

Biplot analysis revealed that the loadings of principal components for both germination parameters and RGB values varied significantly based on the germination conditions employed. Seeds with high L^* and a^* values generally exhibited higher FGP and faster germination rates. These findings underscore the potential of integrating seed coat color parameters into flax breeding programs and highlight their potential role in improving seed germination and overall seed quality under various stress conditions. Future research could explore the potential relationship between seed coat color and agromorphological or yield-related parameters, utilizing the image processing approach developed in this study.

Data availability

Data is provided within the manuscript or supplementary information files. The datasets generated during and/or analyzed during the current study are available from the corresponding author on reasonable request.

Received: 21 February 2025; Accepted: 26 September 2025
Published online: 03 November 2025

References

1. Vishal, B. & Kumar, P. P. Regulation of seed germination and abiotic stresses by gibberellins and abscisic acid. *Front. Plant. Sci.* **9**, 368905 (2018).
2. Singer, S. D. et al. Identification of differential drought response mechanisms in *Medicago sativa* subsp. *sativa* and *falcata* through comparative assessments at the physiological, biochemical, and transcriptional levels. *Plants* **10**, 2107 (2021).
3. Yang, X. et al. Response mechanism of plants to drought stress. *Horticulturae* **7**, 50 (2021).
4. Wang, X., Song, S., Wang, X., Liu, J. & Dong, S. Transcriptomic and metabolomic analysis of seedling-stage soybean responses to PEG-simulated drought stress. *Int. J. Mol. Sci.* **23**, 6869 (2022).
5. Li, G., Manzoor, M. A., Chen, R., Zhang, Y. & Song, C. Genome-wide identification and expression analysis of *TIFY* genes under MeJA, cold and PEG-induced drought stress treatment in *Dendrobium huoshanense*. *Physiol. Mol. Biol. Plants*. **30**, 527–542 (2024).
6. Li, R., Wu, L., Shao, Y., Hu, Q. & Zhang, H. Melatonin alleviates copper stress to promote rice seed germination and seedling growth via crosstalk among various defensive response pathways. *Plant. Physiol. Biochem*. **179**, 65–77 (2022).
7. Tiryaki, I., Sari, U., Cetin, S. & Acar, O. Improved drought tolerance of EMS mutagenized alfalfa (*Medicago sativa* L.) mutants by in vitro screening at germination stage. *Sci. Rep.* **12**, 1–11 (2022).
8. Reed, R. C., Bradford, K. J. & Khanday, I. Seed germination and vigor: ensuring crop sustainability in a changing climate. *Heredity* **128**, 450–459 (2022).
9. Wang, Y. et al. Regulation of seed germination: ROS, epigenetic, and hormonal aspects. *J. Adv. Res.* **71**, 107–125 (2025).
10. Ellouzi, H. et al. Effect of seed priming with auxin on ROS detoxification and carbohydrate metabolism and their relationship with germination and early seedling establishment in salt stressed maize. *BMC Plant. Biol.* **24**, 1–20 (2024).
11. Liu, H. et al. Versatile mxenzymes scavenging Ros for promotion of seed germination under salt stress. *J. Agric. Food Chem* **72**, 4526 (2024).
12. Finch-Savage, W. E. & Bassel, G. W. Seed vigour and crop establishment: extending performance beyond adaptation. *J. Exp. Bot.* **67**, 567–591 (2016).
13. Arshad, M. S. et al. Thermal stress impacts reproductive development and grain yield in rice. *Plant. Physiol. Biochem.* **115**, 57–72 (2017).
14. Poggi, G. M., Corneti, S. & Aloisi, I. The quest for reliable drought stress screening in tetraploid wheat (*Triticum turgidum* spp.) seedlings: why MDA quantification after treatment with 10% PEG-6000 falls short. *Life* **14**, 517 (2024).
15. Govindaraj, M. M. V. G. Importance of genetic diversity assessment in crop plants and its recent advances: an overview of its analytical perspectives. *Wiley Online Library* (2015).
16. Yilmaz, E. G., Tiryaki, I. & Sari, U. Genetic variation among Einkorn genotypes based on gene targeted functional markers and its possible relationship with drought tolerance at seed germination stage. *Mol. Biol. Rep.* **49**, 7389–7398 (2022).
17. Zeroual, A., Baidani, A. & Idrissi, O. Drought stress in lentil (*Lens culinaris*, Medik) and approaches for its management. *Horticulturae* **9**, 1 (2022).
18. Ismael, A. et al. Genetic variation in drought-tolerance traits and their relationships to growth in *Pinus radiata* D. don under water stress. *Front. Plant. Sci.* **12**, 766803 (2022).
19. Yi, F. et al. Seed germination responses to seasonal temperature and drought stress are species-specific but not related to seed size in a desert steppe: implications for effect of climate change on community structure. *Ecol. Evol.* **9**, 2149–2159 (2019).
20. Zhao, Q. et al. Function of *MYB8* in larch under PEG simulated drought stress. *Sci. Rep.* **14**, 1–17 (2024).
21. Ma, L., Wei, J., Han, G., Sun, X. & Yang, X. Seed osmopriming with polyethylene glycol (PEG) enhances seed germination and seedling physiological traits of *Coronilla varia* L. under water stress. *PLoS One*. **19**, e0303145 (2024).
22. Xiao, S. et al. Exogenous melatonin accelerates seed germination in cotton (*Gossypium hirsutum* L). *PLoS One*. **14**, e0216575 (2019).
23. Hasan, M. M. et al. GABA: a key player in drought stress resistance in plants. *Int. J. Mol. Sci.* **22**, 10136 (2021).
24. Wang, L. et al. Melatonin as a key regulator in seed germination under abiotic stress. *J. Pineal Res.* **76**, e12937 (2024).
25. Yousefi, K., Jamei, R. & Darvishzadeh, R. Exogenous 24-Epibrassinolide alleviates salt stress in Okra (*Abelmoschus esculentus* L.) by increasing the expression of SOS pathway genes (SOS1-3) and *NHX1,4* physiol. *Mol. Biol. Plants*. **30**, 2051–2063 (2024).
26. Shafi, Z. et al. The exogenous application of 24-Epibrassinolide (24-EBL) increases the cd and Pb resilience in *Zea Mays* (L.) by regulating the growth and physiological mechanism. *Appl. Biochem. Biotechnol.* **196**, 3949–3973 (2024).
27. Gou, Z., Wang, X. & Wang, W. Evolution of neurotransmitter gamma-aminobutyric acid, glutamate and their receptors. *Zool. Res.* **33**, (2013).
28. Ramos-Ruiz, R., Poirot, E. & Flores-Mosquera, M. GABA, a non-protein amino acid ubiquitous in food matrices. *Cogent Food Agric.* **4**, 1456 (2018).
29. Renault, H. et al. GABA accumulation causes cell elongation defects and a decrease in expression of genes encoding secreted and cell wall-related proteins in *Arabidopsis Thaliana*. *Plant. Cell. Physiol.* **52**, 894–908 (2011).
30. Carillo, P. GABA shunt in durum wheat. *Front. Plant. Sci.* **9**, 316467 (2018).
31. Podlešáková, K., Ugena, L., Spíchal, L. & Doležal, K. De Diego, N. Phytohormones and polyamines regulate plant stress responses by altering GABA pathway. *N Biotechnol.* **48**, 53–65 (2019).

32. Gupta, P. & Dash, P. K. Molecular details of secretory phospholipase A2 from flax (*Linum usitatissimum* L.) provide insight into its structure and function. *Sci. Rep.* **7**, 1–12 (2017).
33. Mostafavi, K. A study effects of drought stress on germination and early seedling growth of flax (*Linum usitatissimum* L.) cultivars. *Adv. Environ. Biol.* **2011**, 3307–3312 (2011).
34. Mahfouze, H. A., Mahfouze, S. A., El-Enany, M. A. M. & Ottai, M. E. Assessment of flax varieties for drought tolerance. *Annu. Res. Rev. Biol.* **21**, 1–12 (2017).
35. Casa, R., Russell, G., Lo Cascio, B. & Rossini, F. Environmental effects on linseed (*Linum usitatissimum* L.) yield and growth of flax at different stand densities. *Eur. J. Agron.* **11**, 267–278 (1999).
36. Dash, P. K. et al. Genome-wide analysis of drought induced gene expression changes in flax (*Linum usitatissimum*). *GM Crops Food.* **5**, 106–119 (2014).
37. Bauer, P. J., Stone, K. C., Foulk, J. A. & Dodd, R. B. Irrigation and cultivar effect on flax fiber and seed yield in the Southeast USA. *Ind. Crops Prod.* **67**, 7–10 (2015).
38. Cullis, C. *The Basic Botany of the Genus* (Springer, 2011).
39. Gallardo, M. A., Milisich, H. J., Drago, S. R. & González, R. J. Effect of cultivars and planting date on yield, oil content, and fatty acid profile of flax varieties (*Linum usitatissimum* L.). *Int. J. Agron.* **2014**, 150570 (2014).
40. Zare, S., Mirlohi, A., Saeidi, G., Sabzalian, M. R. & Ataii, E. Water stress intensified the relation of seed color with Lignan content and seed yield components in flax (*Linum usitatissimum* L). *Sci. Rep.* **11**, 1–15 (2021).
41. Yadav, B. et al. Integrated omics approaches for flax improvement under abiotic and biotic stress: current status and future prospects. *Front. Plant. Sci.* **13**, 931275 (2022).
42. Paliwal, S. et al. Molecular advances to combat different biotic and abiotic stresses in linseed (*Linum usitatissimum* L.): a comprehensive review. *Genes* **14**, 1461 (2023).
43. Parikh, M. et al. Dietary flaxseed as a strategy for improving human health. *Nutrients* **11**, 1171 (2019).
44. Chhillar, H., Chopra, P. & Ashfaq, M. A. Lignans from linseed (*Linum usitatissimum* L.) and its allied species: Retrospect, introspect and prospect. *Crit. Rev. Food Sci. Nutr.* **61**, 2719–2741 (2021).
45. Yang, K. et al. Genetic analysis of genes controlling natural variation of seed coat and flower colors in soybean. *J. Hered.* **101**, 757–768 (2010).
46. Ochuodho, J. O. & Modi, A. T. Dormancy of wild mustard (*Sisymbrium capense*) seeds is related to seed coat colour. *Seed Sci. Technol.* **36**, 46–55 (2008).
47. Ahmed, K., Khatun, M. M., Haque, M. S., Hossain, M. A. & Sarwar, A. K. M. G. Genotypic variations in morphological and yield attributes in flax (*Linum usitatissimum* L.) under salt stress. *Plant Sci. Today* **11**, 4856 (2024).
48. Tiryaki, I. & Kaplan, S. A. Enhanced germination performance of dormant seeds of *Eragrostis tef* in the presence of light. *Trop. Grassl -Forrajes Trop.* **7**, 244–251 (2019).
49. de Medeiros, A. D. et al. Interactive machine learning for soybean seed and seedling quality classification. *Sci. Rep.* **10**, 1–10 (2020).
50. Michel, B. E. & Kaufmann, M. R. The osmotic potential of polyethylene glycol 6000. *Plant. Physiol.* **51**, 914–916 (1973).
51. Goh, T. Y., Basah, S. N., Yazid, H., Aziz Safar, M. J. & Ahmad Saad, F. S. Performance analysis of image thresholding: Otsu technique. *Measurement* **114**, 298–307 (2018).
52. Lamberta, B. Trigonometry for animation. *Foundation HTML5 Animation JavaScript* 69–101 (2011). https://doi.org/10.1007/978-1-4302-3666-5_4.
53. Plante, T. B. & Cushman, M. Choosing color palettes for scientific figures. *Res. Pract. Thromb. Haemost.* **4**, 176–180 (2020).
54. Zapotoczny, P. & Majewska, K. A comparative analysis of colour measurements of the seed coat and endosperm of wheat kernels performed by various techniques. *Int. J. Food Prop.* **13**, 75–89 (2010).
55. Possobom, M. T. D. F., Ribeiro, N. D., Zemolin, A. E. M. & Arns, F. D. Genetic control of the seed coat colour of middle American and Andean bean seeds. *Genetica* **143**, 45–54 (2015).
56. Mirzaei, M. R. & Rajabi, A. Relationship of seed pericarp color with seed quality in sugar beet (*Beta vulgaris* L. var. *Altissima* Döll). *Genet. Resour. Crop Evol.* **68**, 2093–2105 (2021).
57. Yildiz Tiryaki, G., Cil, A. & Tiryaki I. revealing seed coat colour variation and their possible association with seed yield parameters in common vetch (*Vicia sativa* L.). *Int. J. Agron.* **2016**, 1804108 (2016).
58. Varga, F. et al. How does computer vision compare to standard colorimeter in assessing the seed coat color of common bean (*Phaseolus vulgaris* L)? *J. Cent. Eur. Agric.* **20**, 1169–1178 (2019).
59. Halcro, K. et al. The BELT and phenoseed platforms: shape and colour phenotyping of seed samples. *Plant. Methods.* **16**, 1–13 (2020).
60. Buratto, J. S., Fernandes, C. H. D. S., Rosa, J. C. G., de Vanzo, A. T., Caviglione, J. H. & F. & Use of quantitative colorimetry and visual evaluation for color characterization of triticale seeds after phenol reaction. *J. Seed Sci.* **43**, e202143008 (2021).
61. Sofi, P. A., Khalid, K., Sha, R. S., Zaffar, K. S. S. & Majeed Zargar, K. K, A. S. S. S. A low cost and high throughput spectroscopic method for quantification of seed coat colour differences in plain seeded bean (*Phaseolus vulgaris* L.) germplasm from Western Himalayan Kashmir (2022). https://doi.org/10.21203/RS.3.RS-2244758/V1.
62. León, K., Mery, D., Pedreschi, F. & León, J. Color measurement in *L*a*b** units from RGB digital images. *Food Res. Int.* **39**, 1084–1091 (2006).
63. Forsyth, D. & Ponce, J. Computer vision: a modern approach. *Camera* **693**, 562 (2003).
64. Westland, S., Ripamonti, C. & Cheung, V. Computational colour science using MATLAB®, second edition. *Comput. Colour. Sci. using MATLAB® Second Ed.* https://doi.org/10.1002/9780470710890 (2012).
65. Tai, X., Ren, F., Wu, C. & Kita, K. Image retrieval based on color and texture. In *Proc. - Fifth Mexican Int. Conf. Artif. Intell. MICAI, vol .111* 120 (2006).https://doi.org/10.1109/MICAI.2006.25.
66. Sukmana, S. E. & Rahmanti, F. Z. Blight segmentation on corn crop leaf using connected component extraction and CIELAB color space transformation. In *Proceedings – 2017 International Seminar on Application for Technology of Information and Communication: Empowering Technology for a Better Human Life, iSemantic* 205–208 (2017).
67. Love, J. et al. Graphical statistical software for common statistical designs. *J. Stat. Softw.* **88**, 1–17 (2019).
68. Lesik, S. A. *Applied Statistical Inference with MINITAB®*, Second Edition. *Appl. Stat. Inference MINITAB®, Second Edition* (2018). https://doi.org/10.1201/9780429444951.
69. Ibrahim, E. A. Seed priming to alleviate salinity stress in germinating seeds. *J. Plant. Physiol.* **192**, 38–46 (2016).
70. Basal, O., Szabó, A. & Veres, S. Physiology of soybean as affected by PEG-induced drought stress. *Curr. Plant. Biol.* **22**, 100135 (2020).
71. Li, D. et al. GWAS uncovers differential genetic bases for drought and salt tolerances in Sesame at the germination stage. *Genes* **9**, 87 (2018).
72. Wang, X., Cai, X., Xu, C., Wang, Q. & Dai, S. Drought-responsive mechanisms in plant leaves revealed by proteomics. *Int. J. Mol. Sci.* **17**, 1706 (2016).
73. Zhang, X. et al. Genome-wide identification of gene expression in contrasting maize inbred lines under field drought conditions reveals the significance of transcription factors in drought tolerance. *PLoS One.* **12**, e0179477 (2017).
74. Zhang, C., Shi, S., Wang, B. & Zhao, J. Physiological and biochemical changes in different drought-tolerant alfalfa (*Medicago sativa* L.) varieties under PEG-induced drought stress. *Acta Physiol. Plant.* **40**, 1–15 (2018).
75. Basal, O., Szabó, A. & Veres, S. PEG-induced drought stress effects on soybean germination parameters. *J. Plant. Nutr.* **43**, 1768–1779 (2020).

76. Nonami, H. Plant water relations and control of cell elongation at low water potentials. *J. Plant. Res.* **111**, 373–382 (1998).
77. Zhou, M. et al. γ-Aminobutyric acid (GABA) priming improves seed germination and seedling stress tolerance associated with enhanced antioxidant metabolism, *DREB* expression, and dehydrin accumulation in white clover under water stress. *Front. Plant. Sci.* **12**, 776939 (2021).
78. Kintl, A. et al. Effect of seed coating and PEG-induced drought on the germination capacity of five clover crops. *Plants* **10**, 724 (2021).
79. Bajji, M., Lutts, S. & Kinet, J. M. Physiological changes after exposure to and recovery from polyethylene glycol-induced water deficit in callus cultures issued from durum wheat (*Triticum durum* Desf.) cultivars differing in drought resistance. *J. Plant. Physiol.* **156**, 75–83 (2000).
80. Tang, J., Li, M., Mao, P. & Jiang, Y. Effects of Gamma-Aminobutyric acid on seed germination, ion balance, and metabolic activity in perennial ryegrass under salinity stress. *J. Plant. Growth Regul.* **41**, 1835–1844 (2022).
81. Dong, Z. et al. Exogenous γ-Aminobutyric acid can improve seed germination and seedling growth of two cotton cultivars under salt stress. *Plants* **13**, 82 (2023).
82. Wang, X. et al. Gamma-aminobutyric acid (GABA) releases seed dormancy by orchestrating abscisic acid and Gibberellin metabolism and signaling. *BMC Plant. Biol.* **25**, 1–16 (2025).
83. Khan, M. I. R. et al. Role of GABA in plant growth, development and senescence. *Plant. Gene*. **26**, 100283 (2021).
84. Li, L., Dou, N., Zhang, H. & Wu, C. The versatile GABA in plants. *Plant Signal. Behav.* **16**, 4523 (2021).
85. Nicolás-García, M. et al. An overview of instrumented indentation technique for the study of micromechanical properties in food: A case study on bean seed coat. *Biosyst Eng.* **204**, 377–385 (2021).
86. Oh, S., Ahn, E., Shi, A., Mou, B. & Park, S. Genome-wide association studies in lettuce reveal the interplay of seed age, color, and germination under high temperatures. *Sci. Rep.* **15**, 1–12 (2025).
87. Xie, J. et al. Seed color represents salt resistance of alfalfa seeds (*Medicago sativa* L.): based on the analysis of germination characteristics, seedling growth and seed traits. *Front. Plant. Sci.* **14**, 1104948 (2023).
88. Karami, S., Sabzalian, M. R., Rahimmalek, M., Saeidi, G. & Ghasemi, S. Interaction of seed coat color and seed hardness: an effective relationship which can be exploited to enhance resistance to the safflower fly (*Acanthiophilus helianthi*) in *Carthamus* spp. *Crop Prot.* **98**, 267–275 (2017).
89. Abtahi, M., Mirlohi, A., Sharif-Moghaddam, N. & Ataii, E. Revealing seed color variation and their possible association with yield and quality traits in a diversity panel of flax (*Linum usitatissimum* L). *Front. Plant. Sci.* **13**, 1038079 (2022).
90. Zare, S. et al. Water stress and seed color interacting to impact seed and oil yield, protein, mucilage, and secoisolariciresinol diglucoside content in cultivated flax (*Linum usitatissimum* L). *Plants* **12**, 1632 (2023).
91. Fioreze, A. C., da Konkol, C. L., Spanholi, A. C. B., Fioreze, S. L. & D. C. & Evidence of maternal effect on the inheritance of flax (*Linum usitatissimum* L.) seed coat color. *Crop Breed. Appl. Biotechnol.* **23**, e449423210 (2023).
92. Patel, K. P. et al. A review on flax seed: a legume for longevity. *J. Pharm. Res. Int.* **33**, 107–122 (2021).
93. Abtahi, M. & Mirlohi, A. Quality assessment of flax advanced breeding lines varying in seed coat color and their potential use in the food and industrial applications. *BMC Plant. Biol.* **24**, 1–17 (2024).
94. Asgarinia, P. et al. Selection criteria for assessing drought tolerance in a segregating population of flax (*Linum usitatissimum* L). *Can. J. Plant. Sci.* **97**, 424–437 (2016).
95. Saeidi, G. & Rowland, G. G. The effect of temperature, seed colour and linolenic acid concentration on germination and seed vigour in flax. *Can. J. Plant. Sci.* **79**, 315–319 (2011).
96. Chen, R. et al. Gene-to-metabolite network for biosynthesis of lignans in MeJA-elicited *Isatis Indigotica* hairy root cultures. *Front. Plant. Sci.* **6**, 152204 (2015).

Acknowledgements

We would like to thank the Edirne Agricultural Research Institute (Türkiye) for providing the flax varieties. We would like to thank Taner ÇETİN, General Manager of Integra Hydraulics and Automation (Türkiye), for his assistance in the design and production of the photography booth. We would like to thank Yunus Emre ÇELİK, İlkay KAL and Tugay SOLMAZ from AugeLab R&D Tech. Inc. (Türkiye) for their help on seed image analysis.

Author contributions

S.C: Performed and analyzed the germination experiments, conducted image processing and analysis, constructed figures, plots and biplots, and drafted the manuscript. I.T: Conceived the study, secured financial support, designed the experiments, interpreted the data, evaluated the tables and figures, revised and edited the manuscript.

Competing interests

The authors declare no competing interests.

Additional information

Supplementary Information The online version contains supplementary material available at https://doi.org/10.1038/s41598-025-22277-8.

Correspondence and requests for materials should be addressed to I.T.